View metadata, citation and similar papers at core.ac.uk

brought to you by CORE

provided by Elsevier - Publisher Connector

Available online at www.sciencedirect.com

ScienceDirect

Procedia Materials Science 12 (2016) 130 – 135

Procedia Materials Science

www.elsevier.com/locate/procedia

6th New Methods of Damage and Failure Analysis of Structural Parts [MDFA]

Optical modeling of microcrystalline silicon deposited by plasma-enhanced chemical vapor deposition on low-cost iron-nickel substrates for photovoltaic applications

Z. Mrázková[a,b,*], K. Postava[a,c], A. Torres-Rios[b], M. Foldyna[b], P. Roca i Cabarrocas[b], and J. Pištora[a]

[a]*Nanotechnology Centre, VSB – Technical University of Ostrava, 17. listopadu 15, Ostrava – Poruba 708 33, Czech Republic*
[b]*Laboratoire de Physique des Interfaces et des Couches Minces, CNRS, École Polytechnique, Palaiseau 91128, France*
[c]*Institute of Physics, VSB – Technical University of Ostrava, 17. listopadu 15, Ostrava – Poruba 708 33, Czech Republic*

Abstract

This paper deals with the optical modeling of thin hydrogenated microcrystalline silicon films grown on flexible low-cost iron-nickel alloy substrates by low-temperature (175 °C) plasma-enhanced chemical vapor deposition. This material serves as the absorber in solar cells and hence it has direct impact on the resulting solar cell performance. Since the crystallinity and the material quality of hydrogenated microcrystalline silicon films evolve during the growth, the deposited film is inhomogeneous, with a rather complex structure. Real-time spectroscopic ellipsometry has been used to trace the changing composition of the films. In-situ ellipsometric data taken for photon energies from 2.8 to 4.5 eV every 50 seconds enabled us to study the evolution of the monocrystalline silicon fraction of the hydrogenated microcrystalline silicon films.

© 2016 The Authors. Published by Elsevier Ltd. This is an open access article under the CC BY-NC-ND license (http://creativecommons.org/licenses/by-nc-nd/4.0/).

Selection and peer-review under responsibility of the VŠB - Technical University of Ostrava,Faculty of Metallurgy and Materials Engineering

Keywords: In-situ ellipsometry; optical modeling; thin films; plasma-enhanced chemical vapor deposition; microcrystalline silicon; solar cells.

* Corresponding author. *E-mail address:* zuzana.mrazkova@vsb.cz

2211-8128 © 2016 The Authors. Published by Elsevier Ltd. This is an open access article under the CC BY-NC-ND license (http://creativecommons.org/licenses/by-nc-nd/4.0/).

Selection and peer-review under responsibility of the VŠB - Technical University of Ostrava,Faculty of Metallurgy and Materials Engineering
doi:10.1016/j.mspro.2016.03.023

1. Introduction

Photovoltaic industry is today driven by a constant pressure on the decrease of price per watt to less expensive and more efficient solar cells (Branker et al., 2011). Since the photovoltaic module cost depends on the total manufacturing cost of the module (Razykov et al., 2011), innovations leading to the reduction of the solar panel cost and the increase of the energy conversion efficiency are needed. This requires substantial effort towards searching for new materials and designs which can push limits of existing solar cells.

The most recent development of complex materials and nanostructures for solar cells requires more effort to be put into their characterization and modeling. The quality of deposited materials can be monitored by characterization of materials and nanostructures during the growth process using e.g. in-situ ellipsometry [(Kumar et al., 1986), (Jellison Jr. et al., 1993), (Layadi et al., 1995), (Collins et al., 2003)]. However, the model for the in-situ characterization is not always straightforward, because dielectric function as well as the surface of the deposited microcrystalline silicon thin film change during the growth [(Matsuda, 2004), (Fujiwara et al., 2002)].

In this work we deal with the optical modeling of a thin hydrogenated microcrystalline silicon (μc-Si:H) film deposited on a flexible low-cost iron-nickel (Fe-Ni) alloy substrate by low-temperature (175 °C) plasma-enhanced chemical vapor deposition (PECVD), which is promising for a low-cost high-efficiency solar cells production [(Torres-Rios et al., 2011), (Djeridane et al., 2007)]. We focused particularly on a closer analysis of the optical model with a special attention dedicated to the study of the impact of the surface roughness layer composition on the quality of the fit.

2. Experiments

2.1. Deposition of microcrystalline silicon thin film

The studied sample of thin μc-Si:H film on a Fe-Ni alloy substrate was deposited in a PECVD rf power system working at 13.56 MHz. The temperature, the rf power, and the pressure were kept during the deposition at 175 °C, 25 W and 4 Torr, respectively. The deposition was realized using a mixture of silicon tetrafluoride (SiF_4) diluted in hydrogen and argon with an H_2/SiF_4 ratio equal to one.

The iron-nickel alloy (called N42) suitable for a PECVD deposition of μc-Si:H is a low-cost flexible industrial steel with 41 at.% of nickel (Torres-Rios et al., 2011). It has a cubic structure with more than 95 % of the surface oriented in the <100> crystallographic direction (Torres-Rios et al., 2011). Although the lattice constants of N42 substrate and silicon are $a_{N42} = 3.59$ Å and $a_{Si} = 5.43$ Å, respectively, the misfit of only 6.4 % can be achieved by rotation of one of the lattices by 45° with respect to the other. Moreover, both these materials have very similar coefficients of thermal expansion in a wide range of temperatures [(ARCELLORMITTAL, 2007), (Mazur and Gasik, 2009)].

2.2. Real-time spectroscopic ellipsometry

A set of 160 ellipsometric spectra (see Fig. 1) measured by the in-situ spectroscopic phase modulated ellipsometer UVISEL (Jobin-Yvon Horiba) during the material deposition was studied. Each spectrum contains 16 points from the range of photon energies between 3 eV and 4.5 eV with the step of 0.1 eV. The integration time was 300 ms and every spectral measurement took about 48 s. The angle of incidence was 71.20° and the standard ellipsometric configuration with angle of 0° for modulator and +45° for analyzer was used.

3. Results and discussion

Each spectrum was modeled using a separate model with free parameters as in Fig. 2. We have started the fitting from the last measured spectrum and proceeded towards the first measured one. The fitted values of parameters from the previous spectrum were used as the initial parameter values for the subsequent one. Figure 2 shows the schematic drawing of the used optical model. Deposited layer consists of a mixture of monocrystalline silicon (c-Si), the reference highly crystallized hydrogenated microcrystalline silicon prepared by PECVD at hydrogen dilution

ratio of $R = [H_2]/[SiH_4] = 50$ (μc-Si:H-R50) (Yuguchi et al., 2012), and void, with the surface roughness layer represented by a mixture of μc-Si:H-R50 and void.

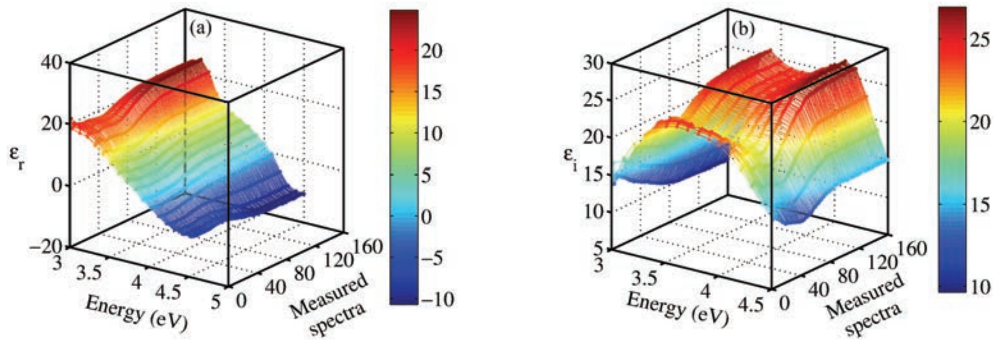

Fig. 1. (a) real and (b) imaginary part of pseudo-dielectric function measured by in-situ ellipsometry during the hydrogenated microcrystalline silicon growth in the PECVD reactor.

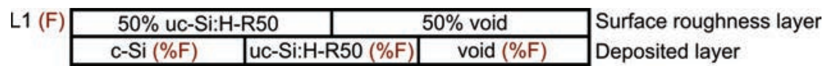

Fig. 2. Schematic drawing of the optical model. Light impinges the material from the top at the incidence angle of 71.20°.

Figure 3 shows dielectric functions of materials used in optical model. Dielectric functions of c-Si and μc-Si:H-R50 were obtained from the literature [(Palik, 1985) and (Yuguchi et al., 2012), respectively]. The dielectric function of hydrogenated amorphous silicon (a-Si:H) prepared at our laboratory and modeled using the Tauc-Lorentz model [(Jellison Jr. and Modine, 1996a), (Jellison Jr. and Modine, 1996b)] is displayed for a comparison.

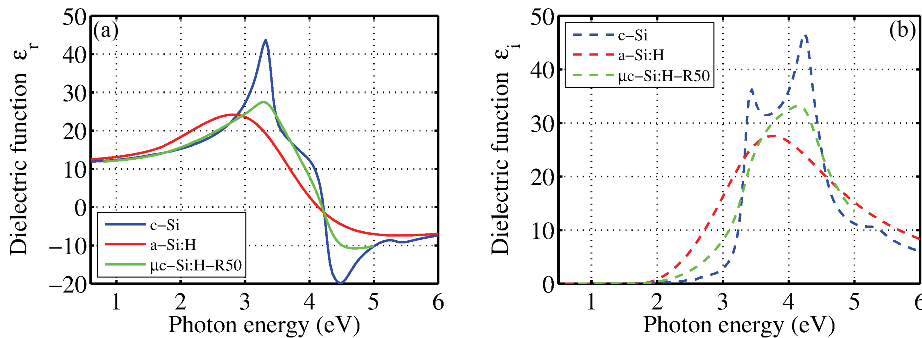

Fig. 3. (a) real and (b) imaginary parts of dielectric functions of monocrystalline silicon (c-Si) from (Palik, 1985), highly crystallized hydrogenated microcrystalline silicon (μc-Si:H-R50) from (Yuguchi et al., 2012), and hydrogenated amorphous silicon (a-Si:H), respectively, used in optical modeling.

The mixture of materials in particular layers was modeled by Bruggeman effective medium approximation (B-EMA) [(Sihvola, 1999), (Aspnes, 1982)]:

$$0 = \sum_j f_j \frac{\varepsilon_j - \varepsilon_{eff}}{\varepsilon_j + \gamma\varepsilon_{eff}}, \tag{1}$$

where ε_{eff} is the dielectric function of the effective medium, ε_j is the dielectric function of the jth inclusion, f_j is the volume fraction of the jth constituent $\left(\sum_j f_j = 1\right)$ and γ is a factor related to the screening and the shape of inclusions (here $\gamma = 2$).

The above mentioned optical model (see Fig. 2) was fitted to the experimental data using the least square algorithm with the following fitting error function χ^2 (Jellison Jr., 1998):

$$\chi^2 = \frac{1}{2M-N-1}\left\{\sum_E \frac{\left[I_S^{meas}(E)-I_S^{mod}(E)\right]^2}{\left[\sigma_{I_S}(E)\right]^2} + \sum_E \frac{\left[I_C^{meas}(E)-I_C^{mod}(E)\right]^2}{\left[\sigma_{I_C}(E)\right]^2}\right\}, \quad (2)$$

where $I_S = \sin2\psi\sin\Delta$ and $I_C = \sin2\psi\cos\Delta$, where ψ and Δ are the ellipsometric angles (Azzam and Bashara, 1987). Superscripts $meas$ and mod stand for the measured and modeled values, respectively. σ represents the estimated measurement error, which is set at a constant value of 0.01. The sum is calculated over the measured spectral interval. M stands for the number of datapoints and N is the number of fitting parameters.

The surface roughness layer is often modeled as an equal mixture of the default material (in our case μc-Si:H-R50) and void (Jellison Jr. et al., 1993). Therefore, we have started with these values in our first model. Below, we will demonstrate that this model is not adapted for all measured spectra. Figure 4(a) (blue spots) shows that values of fitting error function change for different spectra and can reach relatively high values. This means that a model with a fixed composition of surface roughness layer cannot accurately reproduce the whole data set. For instance, the approach with 50 % of μc-Si:H-R50 in the surface roughness layer is suitable only for 34th spectrum and below, since the fitting error function is reasonably small in this region.

To demonstrate the impact of the surface roughness layer composition on the fitted parameters we present in Fig. 4 results for models with the 55 %, 60 %, 65 %, and 70 % of μc-Si:H-R50 in the surface roughness layer, respectively. We can see from Fig. 4(a) that the minimum of the fitting error function shifts with the amount of μc-Si:H-R50 used in the surface roughness layer to a different spectrum.

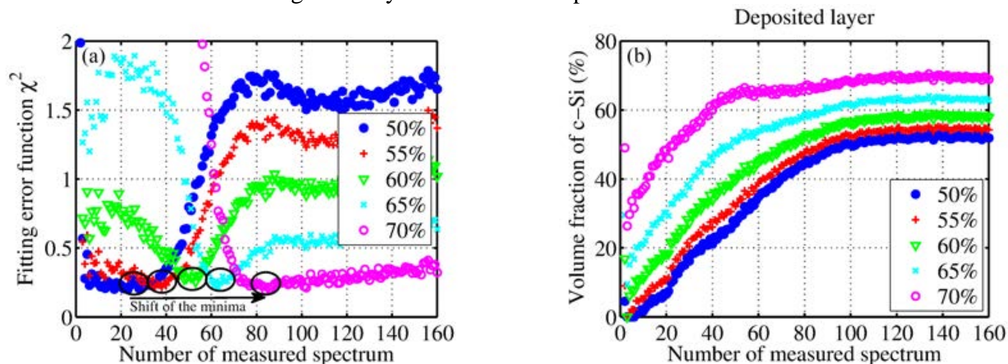

Fig. 4. (a) fitting error function χ^2 and (b) volume fractions of monocrystalline silicon in the deposited layer obtained as the results of the fitting procedure performed for the various amount of the μc-Si:H-R50 in the surface roughness layer, reaching values of 50 %, 55 %, 60 %, 65 %, and 70 %.

Note that not only the fitting error function, but also the volume fraction of monocrystalline silicon in the deposited layer change significantly with the used model [see Fig. 4(b)]. The choice of an inappropriate model can thus lead to inaccurate assessment of the monocrystalline fraction content in the sample.

It can be deduced from the shift of the minimum of fitting error function that the model with 50 % of μc-Si:H-R50 in the surface roughness layer describes accurately the sample at the beginning of the deposition (spectra 2-34), later (spectra 35-46) the model with 55 % of μc-Si:H-R50 suits well, then the model with 60 % of μc-Si:H-R50 corresponds best to the measured data (spectra 47-56), the model with 65 % of μc-Si:H-R50 is appropriate for spectra 57-70, and finally, the model with 70 % of μc-Si:H-R50 must be used from the 71st spectrum to the end of the deposition.

We have demonstrated above that the fitting error function can be significantly reduced by using a suitable model with an appropriate composition of surface roughness layer for different spectra. In order to improve model, we have added the volume fraction of μc-Si:H-R50 in the surface roughness layer to the fitted parameters. Obtained results are shown in Fig. 5 and 6.

Figures 5 and 6 show that using the volume fraction of μc-Si:H-R50 in the surface roughness layer as the floating parameter for each modeled spectrum has improved our model significantly, leading to the continuous trend of all fitted parameters. It can be seen from Fig. 5 that fitting error function (red crosses) is reasonably small and almost constant for all modeled spectra in contrast with the previous case [see Fig. 4(a)]. Moreover, no significant correlations between parameters were observed.

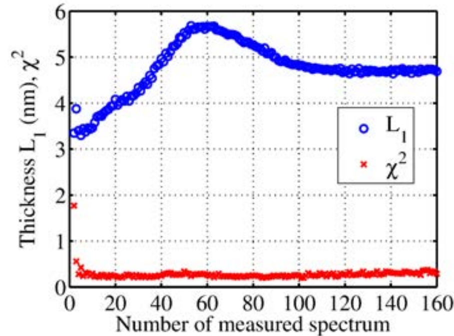

Fig. 5. Fitting error function χ^2 and the thickness of the surface roughness layer L_1 for the model with fitted volume fraction of μc-Si:H-R50 in the surface roughness layer.

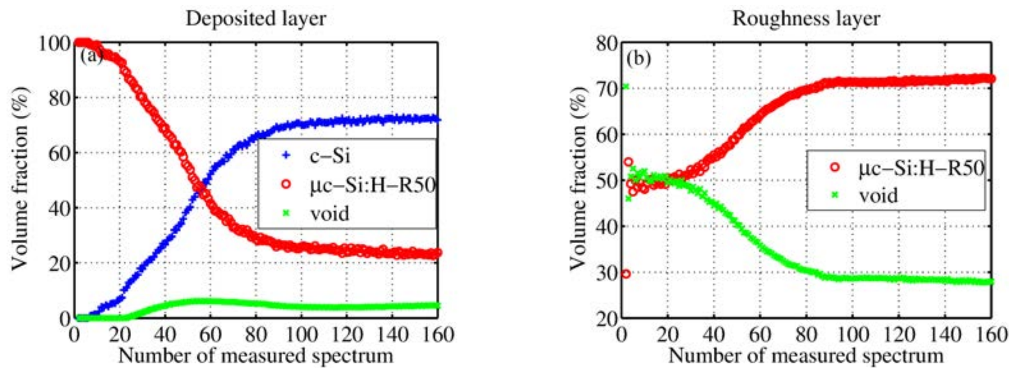

Fig. 6. Best fitted parameters of volume fractions of particular materials in (a) the deposited layer and (b) the surface roughness layer. Values are obtained from the model with fitted volume fraction of μc-Si:H-R50 in the surface roughness layer.

Based on this model we were able to describe the evolution of the material composition in the deposited layer. Figure 6(a) shows the gradual increase of the monocrystalline volume fraction during the material deposition. There is no monocrystalline silicon at the beginning phase of the deposition, then its content gradually increases, reaching its saturation at 70% in the middle of the deposition. After that, the steady growth of silicon with the unchanging composition continues until the end of the deposition.

Note that the material composition of the surface roughness layer changes a lot, starting from amount of μc-Si:H-R50 slightly below 50% at the beginning of the in-situ measurements and reaching over 70% at the end of the deposition [see Fig. 6(b)].

The small increase of the value of fitting error function at the beginning of the deposition (see Fig. 5) indicates the slightly lower accuracy of fit for the first 7 measured spectra. This is because of the presence of a thin incubation layer with a little different composition. This can be solved by adding a-Si:H and the N42 substrate to the model for the very beginning phase of deposition, as presented in our previous paper (Mrázková et al., in press).

4. Conclusions

This paper discusses the detailed optical modeling of the in-situ ellipsometric data measured during the deposition of hydrogenated microcrystalline silicon on Fe-Ni alloy substrate. Focus was on the closer study of the material composition of the surface roughness layer used in the optical model. We demonstrated that this composition has a strong impact on the reliability of resulting fitted parameters as well as the fit accuracy. We showed that the surface roughness layer composition changes a lot during the material growth and cannot be considered constant. Finally, we were able to model the evolution of the material composition of the deposited layer as well as the thickness of the surface roughness layer by adding the μc-Si:H-R50 volume fraction of the surface roughness layer to fitting parameters.

Acknowledgements

The authors thank Pierre-Louis Reydet from Aperam Alloys at Imphy for providing the N42 substrates. Partial financial support from the projects CZ.1.05/1.1.00/02.0070 (IT4Inovations), No. LO1203 "Regional Materials Science and Technology Centre - Feasibility Program", and SP2014/86 is acknowledged.

References

ARCELLORMITTAL, 2007. N42: Controlled-Expansion Alloy.
Aspnes, D.E., 1982. Local-field effects and effective-medium theory: A microscopic perspective. Am J Phys 50, 8.
Azzam, R.M.A., Bashara, N.M., 1987. Ellipsometry and polarized light. North-Holland.
Branker, K., Pathak, M.J.M., Pearce, J.M., 2011. A review of solar photovoltaic levelized cost of electricity. Renew. Sustain. Energy Rev. 15, 4470–4482. doi:10.1016/j.rser.2011.07.104
Collins, R.W., Ferlauto, A.S., Ferreira, G.M., Chen, C., Koh, J., Koval, R.J., Lee, Y., Pearce, J.M., Wronski, C.R., 2003. Evolution of microstructure and phase in amorphous, protocrystalline, and microcrystalline silicon studied by real time spectroscopic ellipsometry. Sol. Energy Mater. Sol. Cells 78, 143–180. doi:10.1016/S0927-0248(02)00436-1
Djeridane, Y., Abramov, A., Roca i Cabarrocas, P., 2007. Silane versus silicon tetrafluoride in the growth of microcrystalline silicon films by standard radio frequency glow discharge. Thin Solid Films 515, 7451–7454. doi:10.1016/j.tsf.2006.11.112
Fujiwara, H., Kondo, M., Matsuda, A., 2002. Microcrystalline silicon nucleation sites in the sub-surface of hydrogenated amorphous silicon. Surf. Sci. 497, 333–340. doi:10.1016/S0039-6028(01)01665-X
Jellison Jr., G.E., 1998. Spectroscopic ellipsometry data analysis: measured versus calculated quantities. Thin Solid Films 313–314, 33–39. doi:10.1016/S0040-6090(97)00765-7
Jellison Jr., G.E., Chisholm, M.F., Gorbatkin, S.M., 1993. Optical functions of chemical vapor deposited thin-film silicon determined by spectroscopic ellipsometry. Appl. Phys. Lett. 62, 3348–3350. doi:10.1063/1.109067
Jellison Jr., G.E., Modine, F.A., 1996a. Parameterization of the optical functions of amorphous materials in the interband region. Appl. Phys. Lett. 69, 371–373.
Jellison Jr., G.E., Modine, F.A., 1996b. Erratum: "'Parameterization of the optical functions of amorphous materials in the interband region'" [Appl. Phys. Lett. 69, 371 (1996)]. Appl. Phys. Lett. 69, 2137–2137. doi:10.1063/1.118155
Kumar, S., Drevillon, B., Godet, C., 1986. Insitu spectroscopic ellipsometry study of the growth of microcrystalline silicon. J. Appl. Phys. 60, 1542–1544. doi:10.1063/1.337289
Layadi, N., Roca i Cabarrocas, P., Drévillon, B., Solomon, I., 1995. Real-time spectroscopic ellipsometry study of the growth of amorphous and microcrystalline silicon thin films prepared by alternating silicon deposition and hydrogen plasma treatment. Phys. Rev. B 52, 5136–5143. doi:10.1103/PhysRevB.52.5136
Matsuda, A., 2004. Microcrystalline silicon.: Growth and device application. J. Non-Cryst. Solids, Proceedings of the 20th International Conference on Amorphous and Microcrystalline Semiconductors 338–340, 1–12. doi:10.1016/j.jnoncrysol.2004.02.012
Mazur, A.V., Gasik, M.M., 2009. Thermal expansion of silicon at temperatures up to 1100 °C. J. Mater. Process. Technol. 209, 723–727. doi:10.1016/j.jmatprotec.2008.02.041
Mrázková, Z., Torres-Rios, A., Ruggeri, R., Foldyna, M., Postava, K., Pištora, J., Roca i Cabarrocas, P., in press. In-situ spectroscopic ellipsometry of microcrystalline silicon deposited by plasma-enhanced chemical vapor deposition on flexible Fe–Ni alloy substrate for photovoltaic applications. Thin Solid Films. doi:10.1016/j.tsf.2014.06.009
Palik, E.D. (Ed.), 1985. Handbook of optical constants of solids. Academic press, New York.
Razykov, T.M., Ferekides, C.S., Morel, D., Stefanakos, E., Ullal, H.S., Upadhyaya, H.M., 2011. Solar photovoltaic electricity: Current status and future prospects. Sol. Energy, Progress in Solar Energy 1 85, 1580–1608. doi:10.1016/j.solener.2010.12.002
Sihvola, A.H., 1999. Electromagnetic Mixing Formulas and Applications. IET.
Torres-Rios, A., Djeridane, Y., Reydet, P.L., Reyal, J.P., Roca i Cabarrocas, P., 2011. Epitaxial Growth of Crystalline Silicon on N42 Alloys by PECVD at 175 °C for Low Cost and High Efficiency Solar Cells, in: EU PVSEC Proceedings. Presented at the 26th European Photovoltaic Solar Energy Conference and Exhibition - EU PVSEC 2011, pp. 2435–2438. doi:10.4229/26thEUPVSEC2011-3DO.7.1
Yuguchi, T., Kanie, Y., Matsuki, N., Fujiwara, H., 2012. Complete parameterization of the dielectric function of microcrystalline silicon fabricated by plasma-enhanced chemical vapor deposition. J. Appl. Phys. 111, 083509. doi:10.1063/1.4704158